A DISCRETE ELEMENT ANALYSIS OF COHESIVE GRANULAR BULK SOLID MATERIALS

LIZ I. DEL CID[1] AND GRAHAM MUSTOE[2]

Colorado School of Mines
College of Computational Sciences and Engineering
Mechanical Engineering Department
1610 Illinois Street
Golden, Colorado 80401
[1]ldelcid@mymail.mines.edu, [2]gmustoe@mines.edu

Key words: Granular Materials, DEM, Contact Problems.

Abstract. In bulk handling applications, such as conveying and storage, understanding the effect cohesion has upon the flow-ability of particulate systems at the macroscopic scale is crucial in increasing the avenues of operation unit design improvements and handling scenarios of industrial operational units. This research provides a better understanding of the role cohesion has on the flow-ability of bulk solids materials through the development, implementation and application of a macroscopic elasto-plastic adhesive (MEPA) contact model within an open source HPC general purpose Discrete Element Method (DEM) computer code.

This investigation proposed a DEM history dependent particle-particle MEPA contact model that accounts for both elastic and plastic contact deformations and adhesive attractions. The research tasks are focused in three major areas: 1) DEM applications for the analysis of cohesive bulk solids, 2) modeling stress history dependency of cohesive strength, and 3) the prediction of flow properties in test applications that are comparable to experimental results. The MEPA model applied herein is a three branched non-linear contact model that simulates the virgin compaction loading, unloading/reloading and adhesion behavior of a particulate solid.

1 INTRODUCTION

For a given bulk handling application, adequately capturing the DEM simulated behavior of cohesive solids is crucial when evaluating its handle-ability. Characterization of bulks solids is required for the reliable design and operation of industrial processes related to the physical storage and handling units of granular materials. The movement of granular matter which exhibits "sticky" or cohesive phenomena gives rise to a wide variety of different flow behaviors. The changing contact networks and stress distributions produce large fluctuations of forces and reorganization of the contacts. The added influence of cohesive forces creates a challenge in predicting the macroscopic flow behavior of a material. Numerical simulation DEM studies conducted with the industry accepted cohesive models show discrepancies between the bulk responses observed in physical tests and those predicted in numerical simulations. The research conducted provides a method for evaluating cohesive strength history conditions for the purpose of providing a tool that can be used within the engineering design of industrial storage and handling systems of frictional-adhesive particulate solids.

2 FLOW MODELING OF COHESIVE BULK SOLIDS WITH THE MACRO ELASTO-PLASTIC ADHESIVE (MEPA) MODEL

The MEPA cohesive model simulates the elastic and plastic regimes. It is capable of modeling material yielding through hysteresis and steady-state flow. This section describes the details of the contact duration with cohesive attraction for each particle contact.

2.1 The MEPA Cohesive Model

The flow behavior of bulk solids under large deformations and displacements is difficult to model with a particle-particle force law that is solely based upon micro-mechanical considerations. The proposed model uses a maximum force-based failure criterion. It determines the maximum displacement of the contact with a material stiffness described by the material's tensile strength, elastic modulus and Poisson's ratio. The novel aspect of this MEPA model is that material behavior is described by macro and micro-mechanics such as the material yield strength and physical properties. This model simulates the mechanical behavior of material physical data in a shear test rather than the micro and molecular mechanics laws. It simulates the results from the physical testing used to determine the parameters of the Mohr-Coulomb shear failure criterion and complements studies in cohesive, frictional bulk solids for micro and macro-models of different materials [1-7].

In the implementation of the MEPA model within the DEM algorithm non-uniform sized spherical particles are used throughout. The material roughness is mimicked with a rolling resistance model that applies additional torques and resistances [8]. In this work, the cohesive bond strength is viewed as a fundamental material parameter and used to numerically resolve macro-mechanical behaviors experimentally observed and described by the Mohr-Coulomb theory within flow property tests.

2.2 Particle Contact Constitutive Model

The relationship between the interaction force and the normal overlap of two rigid DEM particles is established to simplify the contact mechanics. The force-overlap diagram for this model is shown in Figure 1. The MEPA model takes into account plastic contact deformation and cohesive attraction. As two particles are pressed together the particle contact undergoes elastic and plastic deformations. As they continue to be pressed together the pull-off force increases with the increase of the plastic contact area.

The loading, unloading/re-loading and cohesive branches in the MEPA model are represented by four parameters: the virgin loading stiffness parameter k_1, the unloading and reloading stiffness parameter k_2, the cohesive stiffness parameter k_{adh} and the index parameter n, controlling the nonlinear force-displacement response of the system [4-6]. In the initial loading of the contact, the force increases with stiffness k_1. A linear viscous damping dash-pot is used to dissipate energy during contact. Cohesion between the contacts is represented by cohesive stiffness k_{adh}, which allows for attractive forces controlled by a limiting force f_{min}. Note, when $n = 1$, the model becomes linear and is represented by the branched model of Figure 1a. If k_1 is set equal to k_2, the model is reduced to the linear or Hertzian contact model previously discussed. Each branch can be expressed by the following sets of bounding equations:

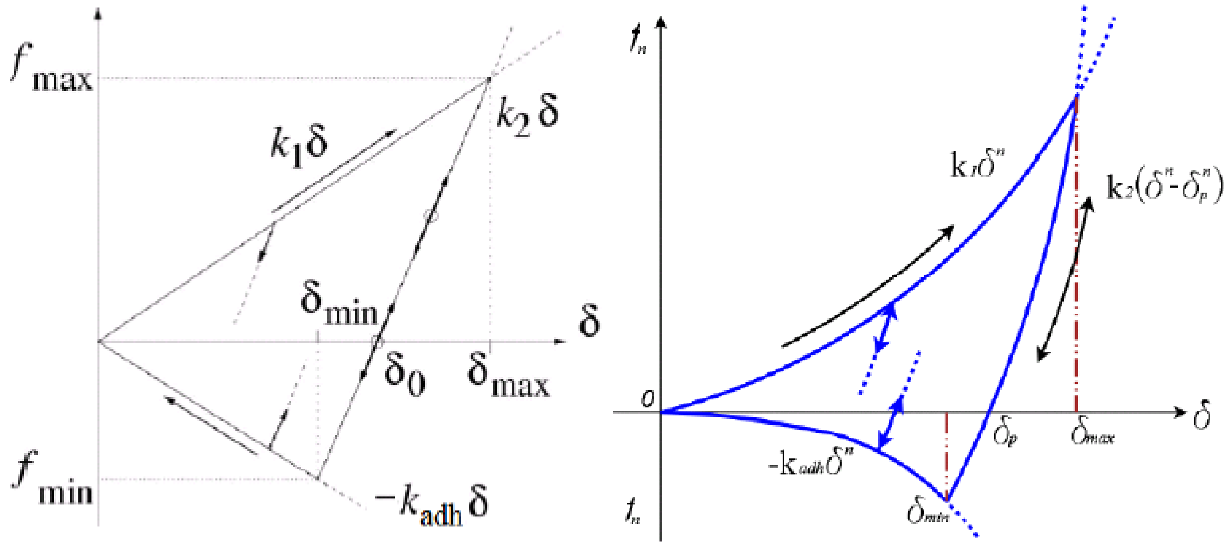

(a) Linear MEPA cohesive contact law. **(b)** Non-linear MEPA cohesive contact law.

Figure 1: Different MEPA contact models from [9].

$$f_1(\delta) = k_1\delta^n \tag{1}$$

$$f_2(\delta) = k_2\left(\delta^n - \delta_p^n\right) \tag{2}$$

$$f_3(\delta) = -k_{adh}\delta^n \tag{3}$$

where $f_1(\delta)$ represents the virgin loading branch, $f_2(\delta)$ the re/unloading branch, and $f_3(\delta)$ the cohesive branch. The branched relationship as a whole can be expressed as:

$$f_{hys} = \begin{cases} f_1(\delta) & if \quad f_2(\delta) \geq f_1(\delta) \\ f_2(\delta) & if \quad f_1(\delta) > f_2(\delta) > f_3(\delta) \\ f_3(\delta) & if \quad f_3(\delta) \geq f_2(\delta) \end{cases} \tag{4}$$

The normal force on particle i is described by:

$$\mathbf{f}_0^n = -\gamma_n \mathbf{v}_n + f_{hys}\mathbf{n} \tag{5}$$

with the normal direction unit vector $\hat{n}$ directed from the center of particle j to particle i. The variable $\mathbf{v}_n$ describes the normal relative velocity of the particle and γ_n the viscous dissipation coefficient. The tangential force includes dissipation due to Coulomb friction and tangential elasticity that allows for stick-slip behavior at the contact level [1, 6, 7]. The tangential force is related to the normal force via Coulomb's law in equation 6.

$$f^t \leq \mu_s f_{hys} \tag{6}$$

The overall solution of the non-linear DEM problem is obtained by incrementally solving Newton's equations of motion with the MEPA cohesive model.

In this study a value of n = 3/2 is used. This converts the MEPA cohesive model into a nonlinear hysteretic spring contact model. The maximum adhesion is determined by the stiffness parameters and the maximum normal overlap f_{max}. The tangential stiffness is calculated based on the contact stiffness k_t, which is set to the value of k_1. The tangential force is calculated from the product of the tangential stiffness and the tangential displacement, subject to the frictional limit according to Coulomb's law. Following the branches of the MEPA cohesive model, during initial compressive loading, the contact force increases with increasing contact overlap. At the maximum contact overlap, f_{max}, the contact stiffness increases instantaneously to the value k_2. Further loading and un-loading is defined by the force-displacement relation $f = f_2(\delta)$. Elastic unloading to a zero contact force leads to a non-zero contact overlap equal to the maximum plastic contact indentation, $\delta = \delta_p$, which is recorded and updated over the contact lifetime. When the contact overlap is further decreased as the particles separate, the contact force enters the tensile regime. The maximum tensile contact force $f = -k_{adh}\delta_{min}^n$ that the contact can experience corresponds to a contact displacement $\delta = \delta_{min}$. Further unloading in the tensile regime generates a tensile contact force that decreases in accordance with $f = -k_{adh}\delta$. In addition to the loading and unloading branches shown in Figure 1a and b, loading and unloading may also occur within the bounding branches. Any loading stage within the bounding branches loads or unloads elastically in accordance with $f = f_2(\delta)$. [8].

3 DEM SIMULATIONS OF THE MECHANICAL BEHAVIOR OF THE MATERIAL COPPER ORE

This section presents the DEM predictions using the MEPA cohesive model for copper ore and compares it to the experimental data of flow property test Report 11040-1 [9].

3.1 Experimental Behavior of Cohesive Granular Materials

The results of a flow property test for copper ore performed by Jenike & Johanson provided by OCC [10] was used as the mechanical testing material data in this study. The data presented in flow property test Report 11040-1 is used to evaluate the capability of the MEPA cohesive model to simulate the mechanical test data [9].

For this study, the results of Sample 1 are used at 5% and 8% moisture contents (mc). The particle size of copper ore tested is 6.35 mm in diameter with a bulk density of 1042.8-1752.4 kg/m^3 for 5% mc and 1350.4-1797.3 kg/m^3 for 8% mc. The weight density of an individual particle of copper ore Sample 1 is 2481.3 kg/m^3. An image of the physical copper ore material with 8% mc can be seen in Figure 2.

Figure 2: Copper ore material at 8% mc from [9].

3.2 The Testing Model Systems and Methods

In this study experimental data sets obtained with the ring cell shear tester series RST-01 developed by Dietmar Schulze [11, 12] are used to validate and calibrate the DEM simulations [11-14]. The yield locus can be plotted from the measured shear points as seen in Figure 3.

3.3 Numerical DEM Model Parameters

The virtual ring cell shear tester was filled with spherical particles with a truncated Gaussian distribution where the mean particle radius is 3.175 mm, and variation in particle radius is $\pm$10% of the mean particle size. This size variation prevents ordered crystal-like packing. A random insertion method was adopted to provide a random packing of the material. Cohesion between particles is accounted for with the k_{adh} value set to a percentage of unloading/reloading stiffness value in the filling process to allow for the development of a similar packing to the physical cohesive material. Static and rolling frictional values are used to account for the roughness of copper ore and the non-spherical nature of the material. The values of material parameters used in the simulations of 5% mc and 8% mc of copper ore are listed in Table 1. The material properties are representative of copper ore. The material reloading and unloading stiffness, k_2, is derived from the material properties such as Young's Modulus, Poisson's ratio and particle density. The loading stiffness, k_1; is equivalent to $\frac{1}{5}k_2$ as suggested in literature [5, 15]. The cohesive stiffness, k_{adh}, was determined iteratively for the moisture content specified. Finally, the frictional values selected are representative of an abrasive material as copper ore is highly abrasive. All the parameters were kept constant throughout the shearing process.

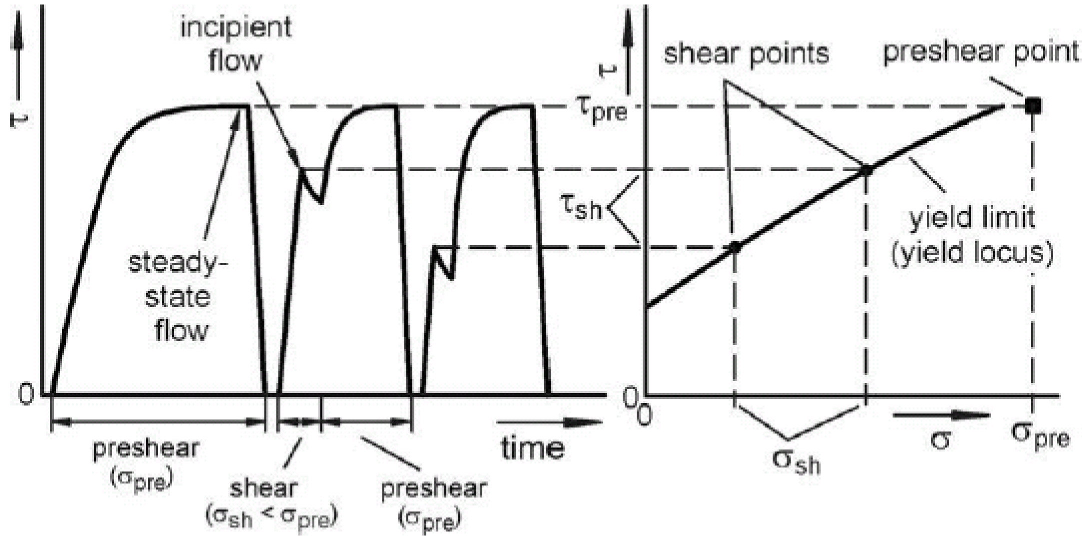

Figure 3: Conceptual shear test procedure of a ring shear tester from [13].

4 MEPA COHESIVE MODEL RESULTS AND DISCUSSIONS

MEPA Cohesive Model Results for Copper Ore Sample 1 with 5% and 8% mc. The yield locus determined through physical experiments for copper ore with a moisture content of 5% and 8% are shown in Figure 4 and Figure 6 respectively. The 6.35 mm diameter material is sheared with a Jenike Shear Tester and serves as the reference case. The ring shearing tests were performed with 6.35 mm diameter material and a cohesive stiffness of $k_{adh} = 3.56 \times 10^8$ Nm for the 5% mc and a cohesive stiffness, $k_{adh} = 5.93 \times 10^8$ Nm for 8% mc. Table 2 shows the determined internal angle of friction of the material as a comparable measurement between tests. The numerical simulation results represent material consolidated at 54.8 kPa for the 5% mc copper ore material conditions and a consolidation of 38.7 kPa for the 8% mc copper ore material conditions listed in Table 1. Figures 5 and 7 show the simulated yield locus for the 5% and 8% mc condition obtained from the shearing cell, respectively, in a comparable graph to the Jenike shear results. The static and rolling frictional values together with the selected cohesive stiffness can account for the variation in the expected result. Additional work should be performed to validate the parameters seen in Table 1 for the consolidation compaction phase in order to gain more confidence in their use. The variation in the shearing points is more evident in lower consolidation pressures.

Discrete Element Method Application of Copper Ore using the MEPA Cohesive Contact Model. To illustrate the application of the MEPA cohesive contact model, a transfer chute DEM simulation was performed with dry copper ore and 8% mc copper ore. The DEM material parameters used for copper ore followed those described in Table 1 with the cohesive stiffness, k_{adh}, set to zero for the dry material simulation. The simulations were performed to observe the mechanical behavior of the simulated copper ore. Figure 8 shows dry copper ore on a transfer belt. It is observed the material is free owing and displays no cohesive agglomerations. In Figure 9, 8% mc copper ore is simulated and compared with the physical material. In Figure 9a, the DEM simulated copper ore displays the mechanical behavior of cohesive materials. Clumps or agglomerations of particles ranging in size from 2.85 mm -

3.49 mm in radius form using the MEPA cohesive contact model and the material parameters described in Table 1. The effective cohesive behavior observed illustrates the capabilities of the MEPA cohesive model to simulate material strength described by physical tests. A more accurate representation is expected with further refinement of the material parameters and DEM particles shapes.

Table 1: Simulation parameters used in the ring shear testers for 5% and 8% mc of copper ore.

	5% mc Copper Ore	8% mc Copper Ore
Poisson's Ratio, υ	0.34	0.34
Young's Modulus, E (GPa)	119	119
Particle Radius, R (mm)	[2.85-3.49]	[2.85-3.49]
Particle Density, ρ (kg/m^3)	2481.3	2481.3
Loading Spring Stiffness, k_1 (N/m)	4.75 x 10^8	4.75 x 10^8
Unloading Spring Stiffness, k_2 (N/m)	2.37 x 10^9	2.37 x 10^9
Cohesive Stiffness, k_{adh} (N/m)	3.56 x 10^8	5.93 x 10^8
Particle Static Friction, μ_s	0.35	0.35
Particle Rolling Friction, μ_r	0.3	0.3
Wall Friction, μ_s	0.0	0.0
Base Friction, μ_s	0.7	0.7
Simulation Time step, Δt (sec)	1.0 x 10^{-7}	1.0 x 10^{-7}

Table 2: Internal frictional angle, φ, for 5% and 8% mc of Copper Ore.

Test	Internal Frictional Angle, φ (degrees) of 5% mc Copper Ore	Internal Frictional Angle, φ (degrees) of 8% mc Copper Ore
Jenike Shear	47.3	46.7
DEM Ring Shear	44.6	44.8

5 CONCLUSIONS

The work contained herein can be broken down into three substantial sections: development of the MEPA cohesive model methodology, modeling of material behavior and its application to simulate large cohesive granular bulk solid systems. The contributions of each of these concepts provide an improved understanding of cohesive flow behavior for the geo-mechanics and bulk material handling communities.

1. *Development of a macro-mechanical cohesive contact model.* The discrete element methodology developed as the MEPA cohesive model uses a maximum force-based failure approach. The model is a three-branch bounded system with stiffness values denoted by k-parameters that describe the following physical effects: compaction (plastic-like deformation), elastic unloading and re-loading of pre-compacted material and adhesive tensile strength of material modeled with cohesion-like behavior.
2. *Modeling material failure via the simulation of physical flow property tests.* To further test the MEPA cohesive model, the effect of moisture content within two copper ore samples was investigated. In application, the MEPA succeeded in illustrating material shearing failure with cohesion by simulating the mechanical behavior of physical data

as seen in Figure 5 and Figure 7. These graphs more closely modeled the observed mechanical behavior of the copper ore material.

3. *Application of the MEPA cohesive contact model in bulk transfer.* The mechanical behavior of copper ore in a transfer system was simulated with the MEPA cohesive contact model. The simulation properly displayed the cohesive agglomerations observed in a sample of the physical copper ore material.

The discrete element method approach to the MEPA cohesive contact model methodology has been successfully implemented and applied to the simulation of copper ore at two different cohesive levels. Initial studies of the available micro cohesive contact models in comparison to the qualitative simulation results obtained from the three-dimensional parallel implementation of the MEPA cohesive constant model illustrates the potential of this new methodology to accurately simulate mechanical behavior in granular bulk solids.

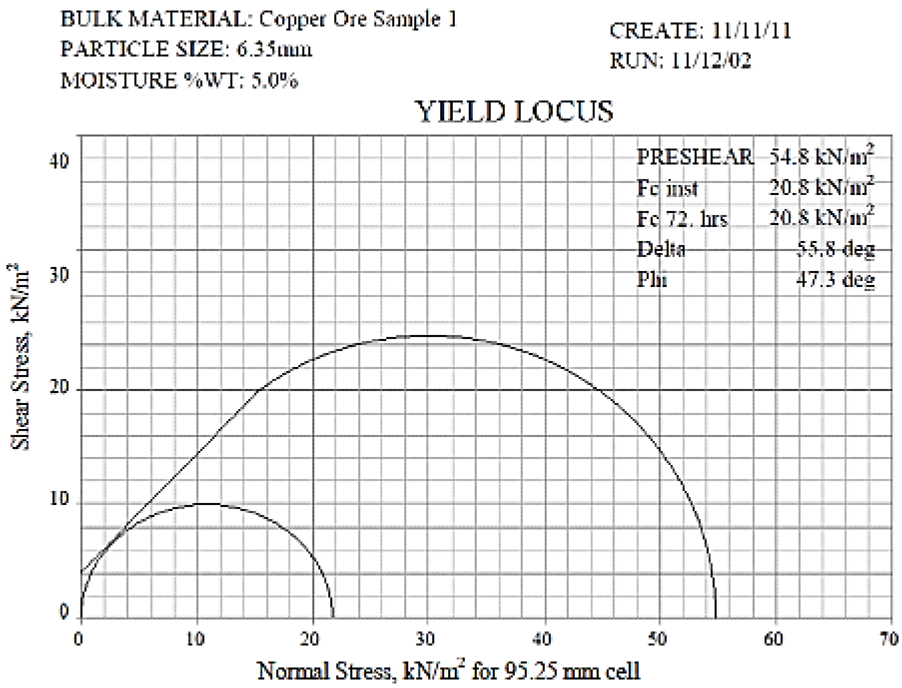

Figure 4: Physical testing results of the loading for Copper Ore Sample 1 at 5% mc [9].

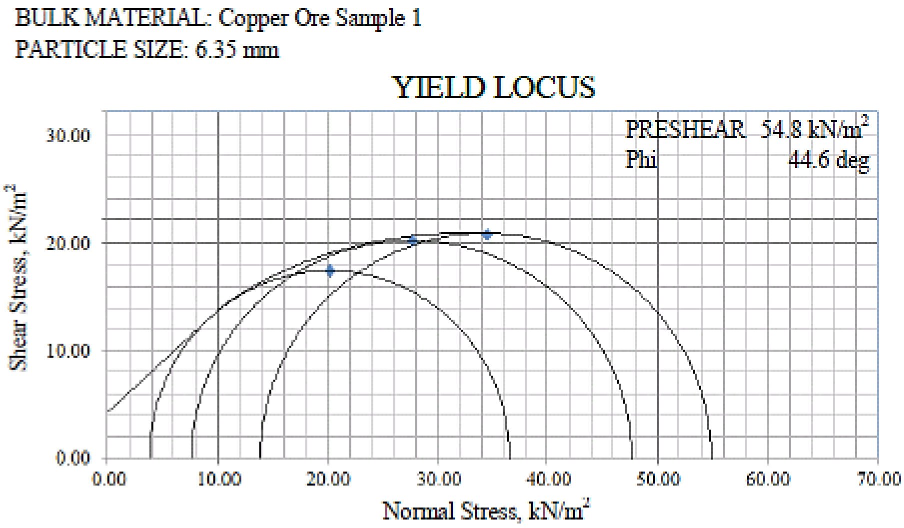

Figure 5: DEM testing results of the loading for Copper Ore Sample 1 at 5% mc with cohesive stiffness, k_{adh} = 3:56 x 10^8 Nm.

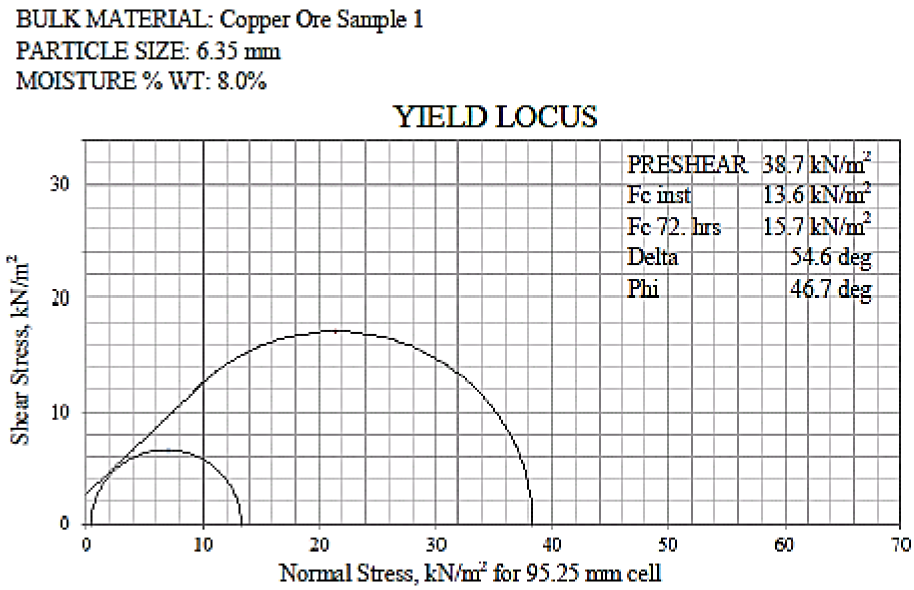

Figure 6: Physical testing results of the loading for Copper Ore Sample 1 at 8% mc [9].

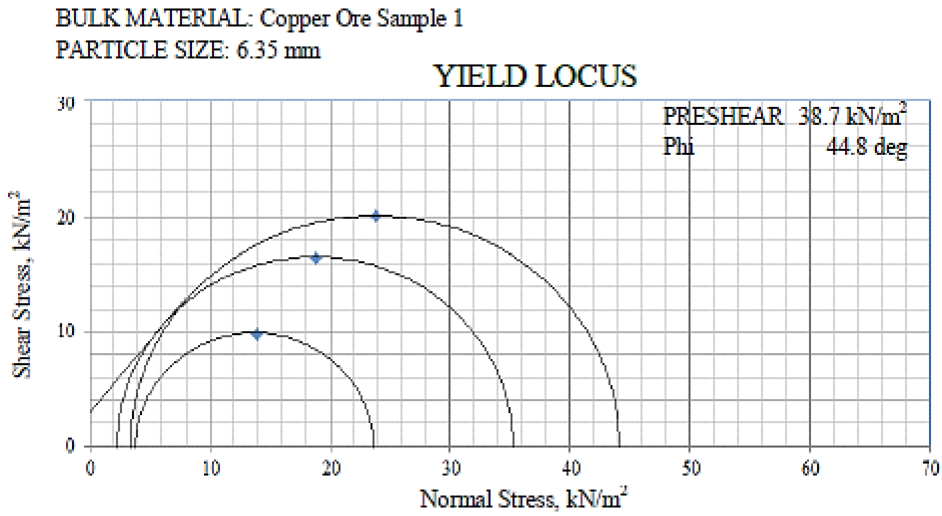

Figure 7: DEM testing results of the loading for Copper Ore Sample 1 at 8% mc with cohesive stiffness, k_{adh} = 5.93 x 10^8 Nm.

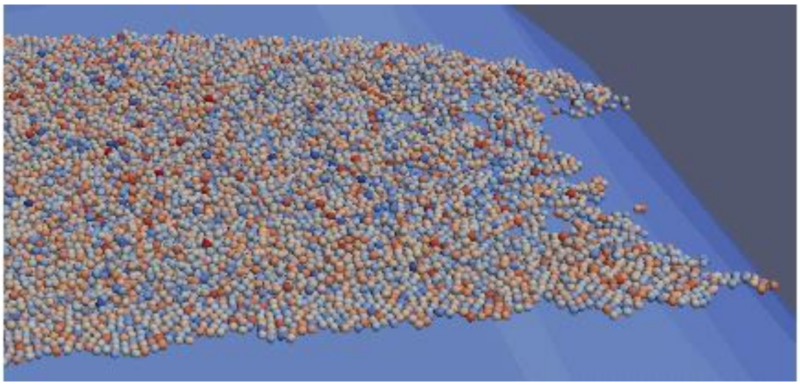

Figure 8: Virtual DEM material representation of dry copper ore on conveying belt.

(a) Physical copper ore material at 8% mc from [9].

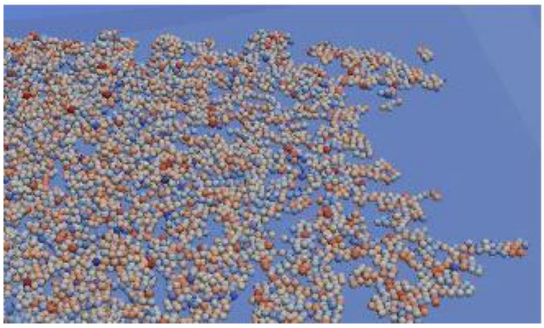

(b) Virtual DEM copper ore material at 8% mc.

Figure 9: DEM simulated material representation of the 8% mc copper ore material.

REFERENCES

[1] Thornton C. and S. J. Antony. Quasi-static shear deformation of a soft particle system. Powder technology, 109(1):179-191, 2000.
[2] D'Addetta G. A., F. Kun, and E. Ramm. On the application of a discrete model to the fracture process of cohesive granular materials. Granular matter, 4(2):77-90, 2002.
[3] Kruyt N. P. and L. Rothenburg. Statistics of the elastic behaviour of granular materials. International Journal of Solids and Structures, 38(28):4879-4899, 2001.
[4] Luding S., M. Latzel, W. Volk, S. Diebels, and H. J. Herrmann. From discrete element simulations to a continuum model. Computer methods in applied mechanics and engineering, 191(1):21-28, 2001.
[5] Tomas J. Assessment of mechanical properties of cohesive particulate solids. Part 1: particle contact constitutive model. Particulate science and technology, 19(2):95-110, 2001.
[6] Luding S. Shear flow modeling of cohesive and frictional fine powder. Powder Technology, 158(1):45-50, 2005.
[7] Luding S., R. Tykhoniuk, and J. Tomas. Anisotropic material behavior in dense, cohesive-frictional powders. Chemical engineering & technology, 26(12):1229-1232,
2003. [20] Ai J., J. F. Chen, M. J. Rotter, and J. Y. Ooi. Assessment of rolling resistance models in discrete element simulations. Powder Technology, 206(3):269-282, 2011.
[8] Thakur S., J. P. Morrissey, J. Sun, J. F. Chen, and J. Y. Ooi. Particle scale modelling of cohesive powders for bulk handling applications. In EDEM Conference, 2011.
[9] Jenike & Johanson, Report 11040-1 : Copper Ore Flow Property Test Report for the Freeport McMoRan Concentrator Feasibility Project as Morenci, Arizona, Overland Conveyor Company Inc. Lakewood, CO 80228, 2011.
[10] Overland Conveyor Company Inc. Lakewood CO 80228. Bulk Material Handling Solutions. http://www.overlandconveyor.com/, 2013.
[11] Schulze D. Development and application of a novel ring shear tester. Aufbereitungs-technik, 35(10):524-535, 1994.
[12] Schulze D. A new ring shear tester for owability and time consolidation measurements. In Proc. 1st International Particle Technology Forum, pages 11-16, 1994.
[13] Schulze D. Flow properties of powders and bulk solids. Braunschweig/Wolfenbu ttel, Germany: University of Applied Sciences, 2006.
[14] Standard ASTM. D6773-02: Standard shear test method for bulk solids using the Schulze ring shear tester, ASTM international.
[15] Zhou Y. C., B. H. Xu, A. B. Yu, and P. Zulli. An experimental and numerical study of the angle of repose of coarse spheres. Powder Technology, 125(1):45-54, 2002.